Supporting Information

Modulating Molecular Aggregates via Nonconjugated Bridges for Enhanced Photocatalytic Hydrogen Evolution

Changzun Jiang[a], Yanting Chen[a], Wentao Yuan[a], Qianqian Li*[a] and Zhen Li*[a,b]

[a] Hubei Key Lab on Organic and Polymeric Opto-Electronic Materials, Department of Chemistry, Wuhan University, Wuhan 430072, China. (http://ligroup.whu.edu.cn/)

[b] College of Chemistry and Chemical Engineering, Hubei University, Wuhan 430062, China

E-mail: liqianqian@whu.edu.cn; lizhen@whu.edu.cn

Materials

Tetrahydrofuran (THF) was dried over and distilled from a K–Na alloy under an atmosphere of dry argon. All solvents were analytical grade and used without further purification. Urea, chloroplatinic acid hexahydrate, bis(di-*tert*-butyl(4-dimethylaminophenyl)phosphine)dichloropalladium(II) ($Pd(Amphos)_2Cl_2$), 4,7-dibromo-5,6-bis(dodecyloxy)benzo[c] [1,2,5] thiadiazole, *N*-bromosuccinimide (NBS), 2-(tributylstannyl)thiophene, 1,4-bis(4,4,5,5-tetramethyl-1,3,2-dioxaborolan-2-yl)benzene, *N*,*N*-diphenyl-4-(4,4,5,5-tetramethyl-1,3,2-dioxaborolan-2-yl)aniline, 3-(2-hexyldecyl)thiophene, 1,3-bis(4,4,5,5-tetramethyl-1,3,2-dioxaborolan-2-yl)benzene and 1,2-bis(4,4,5,5-tetramethyl-1,3,2 dioxaborolan-2-yl)benzene were purchased and used directly as received.

Instruments

^{1}H and ^{13}C NMR spectra were recorded on a Bruker Avance III HD 400 MHz using tetramethylsilane (TMS; δ = 0 ppm) as internal standard. MALDI-TOF spectra were measured on an AB SCIEX MALDI-TOF/TOF 5800. UV-vis spectra were conducted on a Shimadzu UV-2550 spectrometer. Photoluminescence spectra in solution were performed on a Hitachi F-4700 fluorescence spectrophotometer. Photoluminescence spectra, fluorescence lifetimes, and UV–Vis diffuse reflectance spectra (UV–Vis DRS) at the solid state were determined by a FLS980 spectrometer.

Theoretical calculation

Density functional theory (DFT) calculations were performed on Gaussian 16, Revision C01.[1] Molecular structure optimization and frontier molecular orbitas (HOMO and LUMO) was calculated based on PBE1PBE functional with DEF2SVP basis set.[2, 3] Visual pictures were processed with Multiwfn 3.8 and plotted *via* VMD software (version 1.9.3).

Synthesis of polymeric carbon nitride (PCN)

In a typical synthesis, 10 g of urea was calcined at 550 ℃ in air for 2 h at a heating rate of 10 ℃/min^{-1}. The resultant solid as PCN was ground into powder by an agate mortar.

Preparation of PCN/Pt and dye/PCN/Pt systems

PCN powder (500 mg) and $H_2PtCl_6 \cdot 6H_2O$ (40 mg) were added into a mixture of methanol/H_2O solution (120 mL, v/v = 5:1) in a beaker, and the solution was irradiated by a Xe lamp (300 W) for 3 h, PCN/Pt (3.0 wt.% Pt) was obtained by filtration and washed by water for three times. PCN/Pt (100 mg) and each dye (2 mg) were dissolved in a dichloromethane solution (10 mL) and stirred at room temperature in the dark for 3 hours. The solvent was then removed by rotary evaporation to yield the dyes/PCN/Pt.

Characterization of PCN/Pt and dye/PCN/Pt systems

The powder X-ray diffraction patterns were detected by Rigaku SmartLab SE using Cu-Kα radiation from 5° to 80°. Transmission electron microscopy (TEM) was recorded in JEM-F200 transmission electron

microscope. The Fourier transform infrared (FTIR) spectra were recorded on a Thermo Nicolet IS 10 FT-IR spectrometer in the frequency range of 4000-400 cm^{-1}. Fluorescence spectra and lifetimes were determined with an Edinburgh FLS980 spectrometer.

The ultrafast spectroscopic experiments were performed on a commercial spectrometer (TA-100DZ, Time-Tech). The fundamental beam (1030 nm, pulse duration ~290 fs, 100kHz repetition rate, PH2-20W, Light Conversion) was split into two parts. One beam is sent to an optical parametric amplifier (ORPHEUS-HP, Light Conversion) to generate the 400 nm pump pulse. The pump is chopped at a frequency of 500 Hz, and its intensity is attenuated by neutral density filter wheels. The other 800 nm beam is focused into a sapphire crystal to generate a white light probe (450-810 nm), probe pulses are delayed in time with respect to the pump pulses using a motorized translation stage mounted with a retroreflecting mirror. The pump and probe are spatially focused and overlapped on the sample surface.

Photoelectrochemical property

The transient photocurrent and electrochemical impedance spectroscopy (EIS) were obtained in a conventional three-electrode cell by ModuLab XM ECS, using a Pt plate as the counter electrode and an Ag/AgCl (3 M KCl) electrode as the reference electrode. The working electrode was prepared on indium-tin oxide (ITO) glass, which was cleaned by sonication in ethanol and acetone for 30 min and dried at 353 K. The boundary of the ITO glass was protected using Scotch tape. The 5 mg of sample (PCN, PCN/Pt, dye/PCN/Pt) was dispersed in a 0.5 mL solution (480 μL of absolute ethanol and 20 μL of Nafion solution) by sonication to get a slurry. The slurry was spread onto pretreated ITO glass. After air-drying, the Scotch tape was unstuck, and the uncoated part of the electrode was isolated with epoxy resin to get a 1 cm × 1 cm film electrode. A Na_2SO_4 solution (0.5 M) was used as the electrolyte. Before testing, the electrolyte was purged with N_2 to remove dissolved oxygen. EIS was determined over the frequency range of 10^{-2} - 10^6 Hz with an ac amplitude of 10 mV at the open circuit voltage.

Photocatalytic property

Photocatalytic hydrogen evolution arrays were performed in a Pyrex top-irradiation reaction vessel linked to a gas detection system. H_2 production was carried out by dispersing 50 mg of photocatalyst powder in an aqueous solution (100 mL) containing triethanolamine (10 vol.%) as the sacrificial electron donor. The mixture was evacuated several times to remove air completely before irradiation under a 300 W Xe-lamp and a water-cooling filter. The mixture was kept at room temperature by a flow of cooling water. The generated gases were analyzed by gas chromatography equipped with a thermal conductive detector (TCD) with argon as the carrier gas. The apparent quantum yield (AQY) for H_2 evolution was determined at 380 nm, 420 nm, 475 nm, 500 nm, 520 nm, 550 nm, 600 nm, and 650 nm. The AQY values were calculated by the following equation:

$$AQY = \frac{2 \times Number\ of\ H_2}{Number\ of\ incident\ photos} \times 100\% = \frac{2 \times n_{H_2} \times N_A}{S \times P \times t \times \frac{\lambda}{hc}}$$

Where nH_2 is the evolved hydrogen amount (μmol), N_A is the Avogadro constant (6.02×10^{23} mol^{-1}), S is

the illumination area (cm^2), t is the irradiation time (s), *h* is the Plank constant (6.626×10^{-34} J·s), c is the speed of light (3×10^8 m s^{-1}). P and λ are the optical power density (W cm^{-2}) and wavelength (nm) of the monochromatic light, respectively.

Synthesis of organic dyes

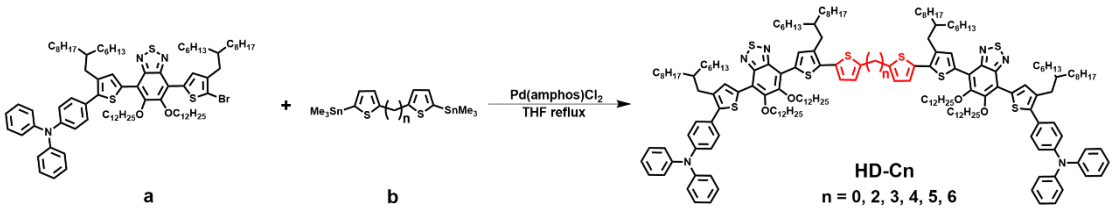

Scheme S1. Synthetic routes of organic dyes

General synthesis of organic dyes Compound a and b were synthesized according to references.[4, 5] Under an atmosphere of nitrogen, a mixture of the compound **a** (2.1 equiv.), **b** (1.0 equiv.), Pd(amphos)Cl_2 (0.1 equiv.) and potassium carbonate (10.0 equiv.) in 20 mL mixed solvent (tetrahydrofuran/water = 10/1) was placed in Schlenk tube and stirred at 80 °C for 12 hours. After being cooled to room temperature, the mixture was poured into water and extracted with dichloromethane for three times. The combined organic layers were dried with anhydrous sodium sulfate. After the solvent was evaporated, the crude products were purified by column chromatography.

HD-C0: A red solid (0.100 g, 82%). ^{1}H NMR (400 MHz, $CDCl_3$) δ 8.45 (s, 2H), 8.38 (s, 2H), 7.41 (d, *J* = 8.5 Hz, 4H), 7.30 (d, *J* = 7.2 Hz, 4H, ArH), 7.28 (d, *J* = 7.1 Hz,, 4H, ArH), 7.21 – 7.11 (m, 16H, ArH), 7.06 (m, 4H, ArH), 4.18 (m, 8H, OCH_2), 2.87 (d, *J* = 7.2 Hz, 4H, CH_2), 2.74 (d, *J* = 7.1 Hz, 4H, CH_2), 2.04 – 1.95 (m, 8H, CH_2), 1.90 – 1.85 (m, 2H, CH), 1.74 (s, 2H, CH), 1.42 – 1.23 (m, 168H, CH_2), 0.87 (m, 36H, CH_3). ^{13}C NMR (101 MHz, $CDCl_3$) δ 151.95, 151.59, 151.09, 150.90, 147.62, 147.07, 140.71, 138.69, 137.33, 137.06, 135.52, 134.57, 134.13, 132.81, 132.22, 131.46, 130.18, 129.33, 128.71, 126.63, 124.67, 123.87, 123.11, 123.06, 117.69, 116.82, 77.24, 74.47, 74.36, 39.21, 38.90, 34.07, 33.58, 33.51, 33.18, 32.03, 31.98, 31.96, 30.50, 30.46, 30.18, 30.15, 29.86, 29.79, 29.75, 29.72, 29.44, 29.40, 26.59, 26.55, 26.50, 26.17, 22.76, 22.72, 14.17, 14.15. MS (MALDI-TOF, m/z): [M]+ calcd for $C_{184}H_{268}N_6O_4S_8$: 2883.88, found 2884.15.

HD-C2: A red solid (0.082 g, 71%). ^{1}H NMR (400 MHz, CDCl3) δ 8.41 (s, 2H, ArH), 8.37 (s, 2H, ArH), 7.45 – 7.39 (m, 4H, ArH), 7.34 – 7.27 (m, 8H, ArH), 7.20 – 7.15 (m, 8H, ArH), 7.15 – 7.10 (m, 4H, ArH), 7.07 (m, 6H, ArH), 6.85 (d, *J* = 3.6 Hz, 2H, ArH), 4.18 (q, *J* = 6.7 Hz, 8H, OCH_2), 3.28 (s, 4H, CH_2), 2.83 (d, *J* = 7.1 Hz, 4H, CH_2), 2.74 (d, *J* = 7.0 Hz, 4H, CH_2), 2.05 – 1.92 (m, 8H, CH_2), 1.90 – 1.79 (m, 2H, CH), 1.75 (d, *J* = 6.4 Hz, 2H, CH), 1.52 – 1.42 (m, 8H, CH_2), 1.36 – 1.20 (m, 160H, CH_2), 0.90 – 0.84 (m, 36H, CH_3).^{13}C NMR (101 MHz, $CDCl_3$) δ 151.83, 151.65, 151.09, 150.95, 147.63, 147.06, 143.90, 140.61, 138.10, 137.30, 134.53, 134.37, 134.06, 133.44, 131.74, 131.51, 130.19, 129.33, 128.74, 125.83, 125.08, 124.66, 123.11, 123.07, 117.52, 117.00, 77.36, 77.25, 77.04, 76.73, 74.40, 74.34, 39.21, 38.91, 33.91, 33.56, 33.51, 33.18, 32.37, 32.03, 31.99, 31.97, 30.49, 30.47, 30.18, 30.15, 29.85, 29.81, 29.80, 29.78, 29.76, 29.74, 29.72, 29.44, 29.40, 26.59, 26.55, 26.50,

26.17, 22.76, 22.74, 22.73, 22.71, 14.19, 14.16, 0.03. [M]+ calcd for $C_{186}H_{272}N_6O_4S_8$: 2911.91, found 2912.48.

HD-C3: A red solid (0.077 g, 84%).^{1}H NMR (400 MHz, $CDCl_3$) δ 8.39 (s, 2H, ArH), 8.36 (s, 2H, ArH), 7.43 – 7.37 (m, 4H, ArH), 7.32 – 7.26 (m, 8H, ArH), 7.19 – 7.14 (m, 8H, ArH), 7.14 – 7.09 (m, 4H, ArH), 7.09 – 7.03 (m, 6H, ArH), 6.82 (d, *J* = 3.6 Hz, 2H, ArH), 4.16 (td, *J* = 7.0, 4.7 Hz, 8H, OCH_2), 2.97 (t, *J* = 7.4 Hz, 4H, CH_2), 2.82 (d, *J* = 7.1 Hz, 4H, CH_2), 2.73 (d, *J* = 7.0 Hz, 4H, CH_2), 2.17 (m, 2H, CH_2), 2.04 – 1.91 (m, 8H, CH_2), 1.87 – 1.79 (m, 2H, CH), 1.77 – 1.69 (m, 2H, CH), 1.48 (m, 8H, CH_2), 1.38 – 1.21 (m, 160H, CH_2), 0.89 – 0.83 (m, 36H, CH_2). ^{13}C NMR (101 MHz, CDCl3) δ 151.80, 151.65, 151.08, 150.94, 147.62, 147.04, 144.86, 140.58, 137.98, 137.29, 134.36, 134.26, 134.03, 133.56, 131.62, 131.50, 130.17, 129.32, 128.74, 125.82, 124.89, 124.65, 123.09, 123.06, 117.47, 117.02, 77.35, 77.23, 77.03, 76.71, 74.33, 39.19, 38.88, 33.88, 33.50, 33.17, 32.00, 31.97, 31.95, 30.46, 30.16, 30.14, 29.83, 29.80, 29.78, 29.75, 29.73, 29.70, 29.42, 29.39, 26.56, 26.53, 26.48, 26.15, 22.75, 22.73, 22.71, 22.70, 14.17, 14.14, 0.01. $[M+H]^+$ calcd for $C_{187}H_{275}N_6O_4S_8$: 2925.93, found 2926.35.

HD-C4: A red solid (0.13 g, 86%).^{1}H NMR (400 MHz, $CDCl_3$) δ 8.39 (s, 2H, ArH), 8.36 (s, 2H, ArH), 7.44 – 7.37 (m, 4H, ArH), 7.33 – 7.27 (m, 8H, ArH), 7.19 – 7.14 (m, 8H, ArH), 7.14 – 7.10 (m, 4H, ArH), 7.06 (m, 6H, ArH), 6.79 (d, *J* = 3.5 Hz, 2H, ArH), 4.16 (td, *J* = 7.1, 4.1 Hz, 8H, OCH_2), 3.00 – 2.86 (m, 4H, CH_2), 2.82 (d, *J* = 7.2 Hz, 4H, CH_2), 2.73 (d, *J* = 7.1 Hz, 4H, CH_2), 1.97 (m, 8H, CH_2), 1.91 – 1.84 (m, 4H, CH_2), 1.85 – 1.79 (m, 2H, CH_2), 1.79 – 1.70 (m, 2H, CH_2), 1.49 (m, 8H, CH_2), 1.37 – 1.22 (m, 160H, CH_2), 0.90 – 0.84 (m, 36H, CH_3). ^{13}C NMR (101 MHz, $CDCl_3$) δ 151.78, 151.65, 151.09, 150.95, 147.63, 147.04, 145.51, 140.58, 137.92, 137.29, 134.39, 134.05, 133.64, 131.56, 131.51, 130.18, 129.32, 128.75, 125.78, 124.66, 124.56, 123.10, 123.07, 117.46, 117.04, 77.35, 77.24, 77.04, 76.72, 74.33, 39.20, 38.87, 33.87, 33.51, 33.16, 32.01, 31.98, 31.96, 31.15, 30.46, 30.17, 30.15, 29.95, 29.84, 29.80, 29.79, 29.76, 29.74, 29.71, 29.43, 29.40, 26.56, 26.54, 26.52, 26.49, 26.16, 22.76, 22.74, 22.72, 22.71, 14.18, 14.16, 14.14, 0.02. [M]+ calcd for $C_{188}H_{276}N_6O_4S_8$: 2939.94, found 2940.33.

HD-C5: A red solid (0.095 g, 79%). ^{1}H NMR (400 MHz, $CDCl_3$) δ 8.38 (s, 2H, ArH), 8.36 (s, 2H, ArH), 7.43 – 7.38 (m, 4H, ArH), 7.32 – 7.26 (m, 8H, ArH), 7.20 – 7.14 (m, 8H, ArH), 7.14 – 7.10 (m, 4H, ArH), 7.08 – 7.03 (m, 6H, ArH), 6.78 (d, *J* = 3.5 Hz, 2H, ArH), 4.16 (m, 8H, OCH_2), 2.88 (t, *J* = 7.6 Hz, 4H, CH_2), 2.81 (d, *J* = 7.2 Hz, 4H, CH_2), 2.73 (d, *J* = 7.1 Hz, 4H, CH_2), 1.97 (m, 8H, CH_2), 1.81 (m, 6H, CH_2), 1.74 (s, 2H, CH_2), 1.49 (m, 10H, CH_2), 1.36 – 1.21 (m, 160H, CH_2), 0.86 (m, 36H, CH_3). ^{13}C NMR (101 MHz, $CDCl_3$) δ 151.77, 151.65, 151.08, 150.95, 147.63, 147.04, 145.85, 140.57, 137.88, 137.29, 134.38, 134.02, 133.94, 133.68, 131.51, 130.17, 129.32, 128.74, 125.76, 124.65, 124.45, 123.09, 123.06, 117.44, 117.04, 77.35, 77.24, 77.03, 76.71, 74.37, 39.19, 38.86, 33.87, 33.52, 33.16, 32.00, 31.97, 31.95, 31.44, 30.46, 30.16, 30.14, 29.83, 29.80, 29.78, 29.75, 29.73, 29.70, 29.43, 29.39, 28.81, 26.54, 26.51, 26.48, 26.15, 22.75, 22.72, 22.69, 14.17, 14.15, 0.01. [M]+ calcd for $C_{189}H_{278}N_6O_4S_8$: 2953.96, found 2954.37.

HD-C6: A red solid (0.089 g, 71%). ^{1}H NMR (400 MHz, $CDCl_3$) δ 8.38 (s, 2H, ArH), 8.35 (s, 2H, ArH), 7.43 – 7.36 (m, 4H, ArH), 7.32 – 7.27 (m, 8H, ArH), 7.19 – 7.14 (m, 8H, ArH), 7.14 – 7.09 (m, 4H, ArH), 7.08 – 7.02 (m, 6H, ArH), 6.77 (d, *J* = 3.5 Hz, 2H, ArH), 4.15 (td, *J* = 7.1, 3.6 Hz, 8H, OCH_2), 2.86 (t, *J* = 7.6 Hz, 4H, CH_2), 2.80 (d, *J* = 7.2 Hz, 4H, CH_2), 2.72 (d, *J* = 7.1 Hz, 4H, CH_2), 1.96 (h, *J* = 7.4 Hz, 8H, CH_2), 1.85 – 1.71 (m, 8H, CH_2), 1.52 – 1.44 (m, 12H, CH_2), 1.34 – 1.20 (m, 160H, CH_2), 0.89 – 0.84 (m, 36H, CH_3). ^{13}C NMR

(101 MHz, $CDCl_3$) δ 151.76, 151.65, 151.08, 150.95, 147.62, 147.03, 146.00, 140.56, 137.85, 137.28, 134.39, 134.01, 133.87, 133.71, 131.48, 130.17, 129.32, 128.74, 125.74, 124.65, 124.39, 123.09, 123.06, 117.43, 117.05, 77.35, 77.23, 77.03, 76.71, 74.37, 39.19, 38.86, 33.86, 33.52, 33.16, 32.00, 31.97, 31.95, 31.59, 30.46, 30.16, 30.14, 29.83, 29.78, 29.75, 29.73, 29.70, 29.43, 29.39, 29.00, 26.54, 26.48, 26.15, 22.74, 22.71, 22.70, 14.17, 14.15. [M]+ calcd for $C_{190}H_{280}N_6O_4S_8$: 2967.97, found 2968.36.

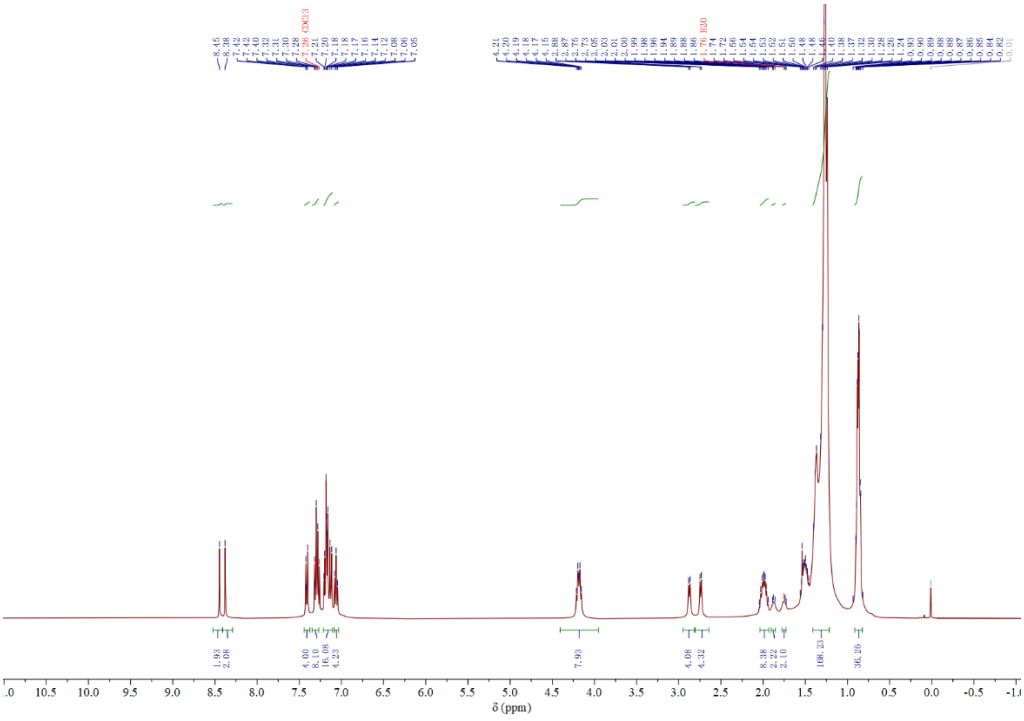

Figure S1. ^{1}H NMR spectrum of HD-C0 (400 MHz, $CDCl_3$).

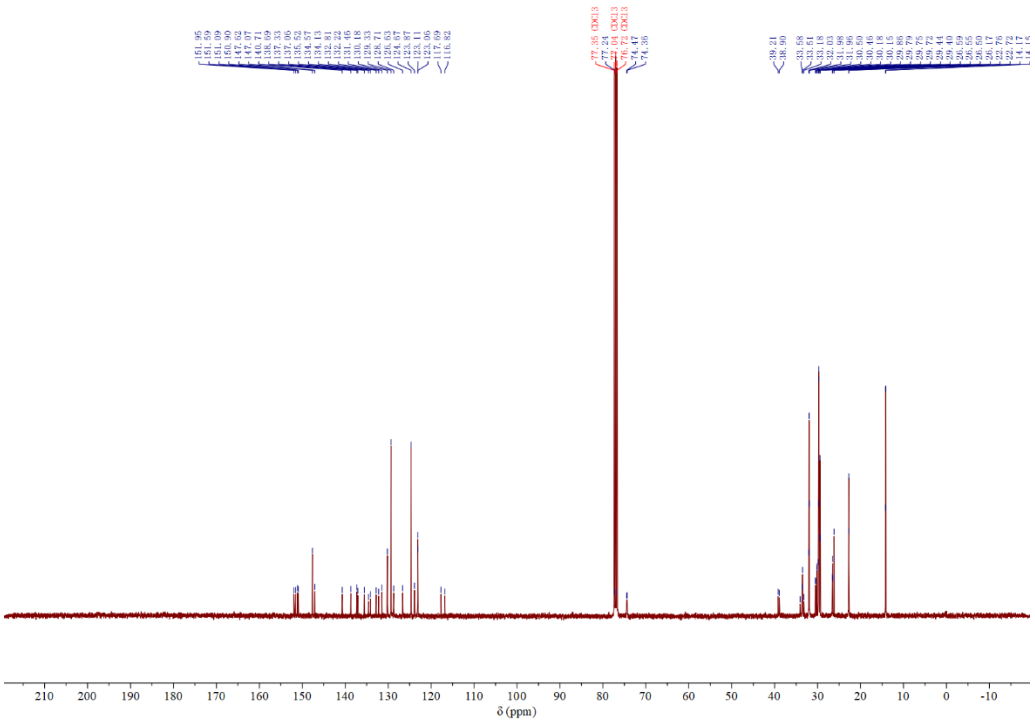

Figure S2. ^{13}C NMR spectrum of HD-C0 (101 MHz, $CDCl_3$).

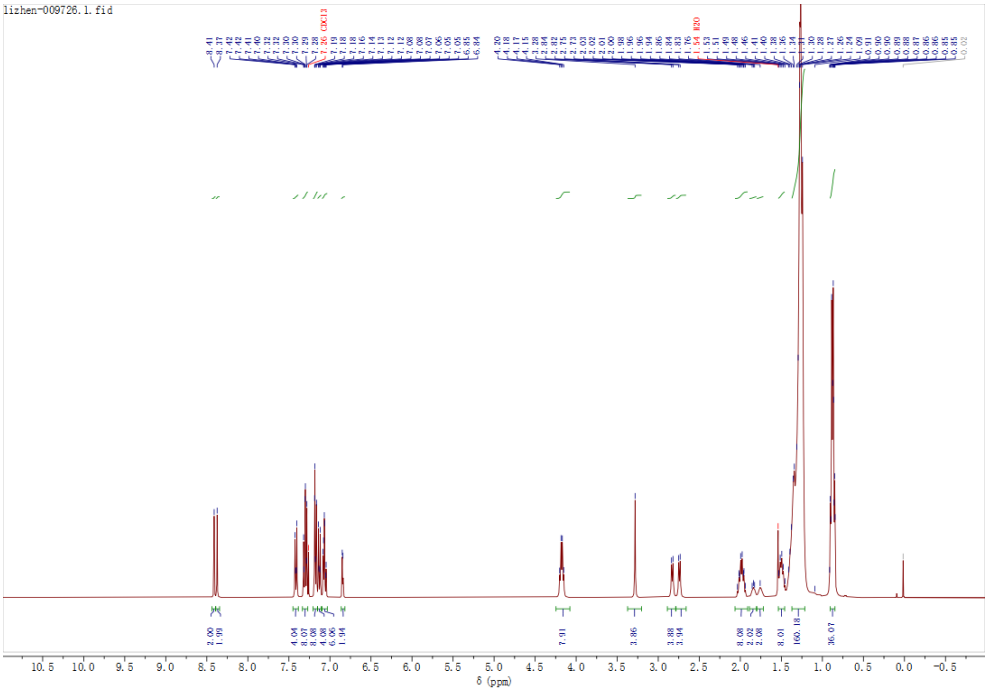

Figure S3. ^{1}H NMR spectrum of HD-C2 (400 MHz, $CDCl_3$).

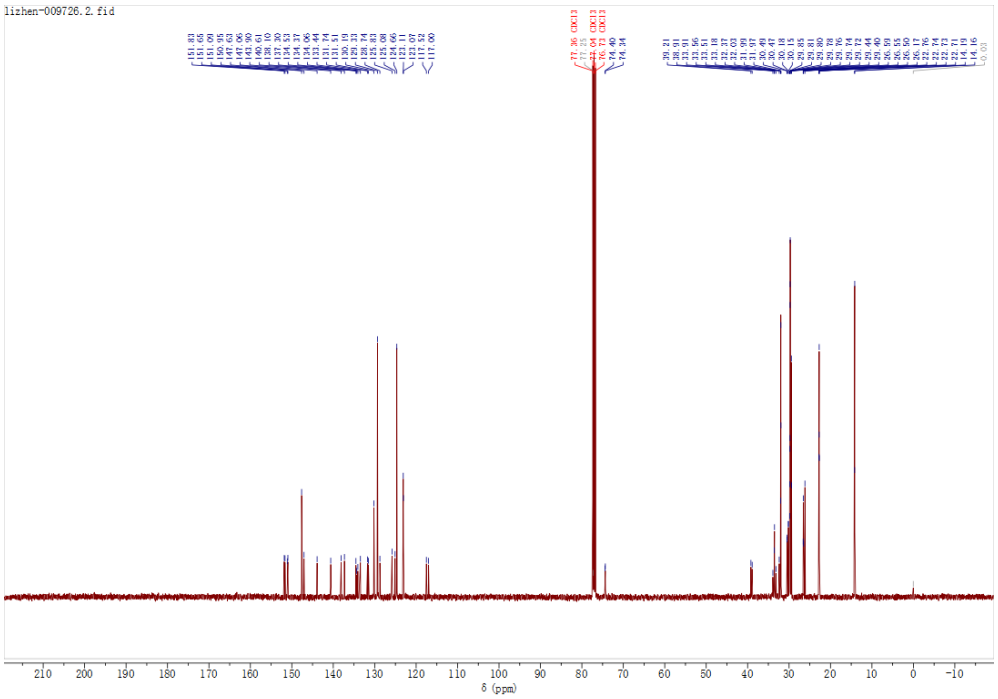

Figure S4. ^{13}C NMR spectrum of HD-C2 (101 MHz, $CDCl_3$).

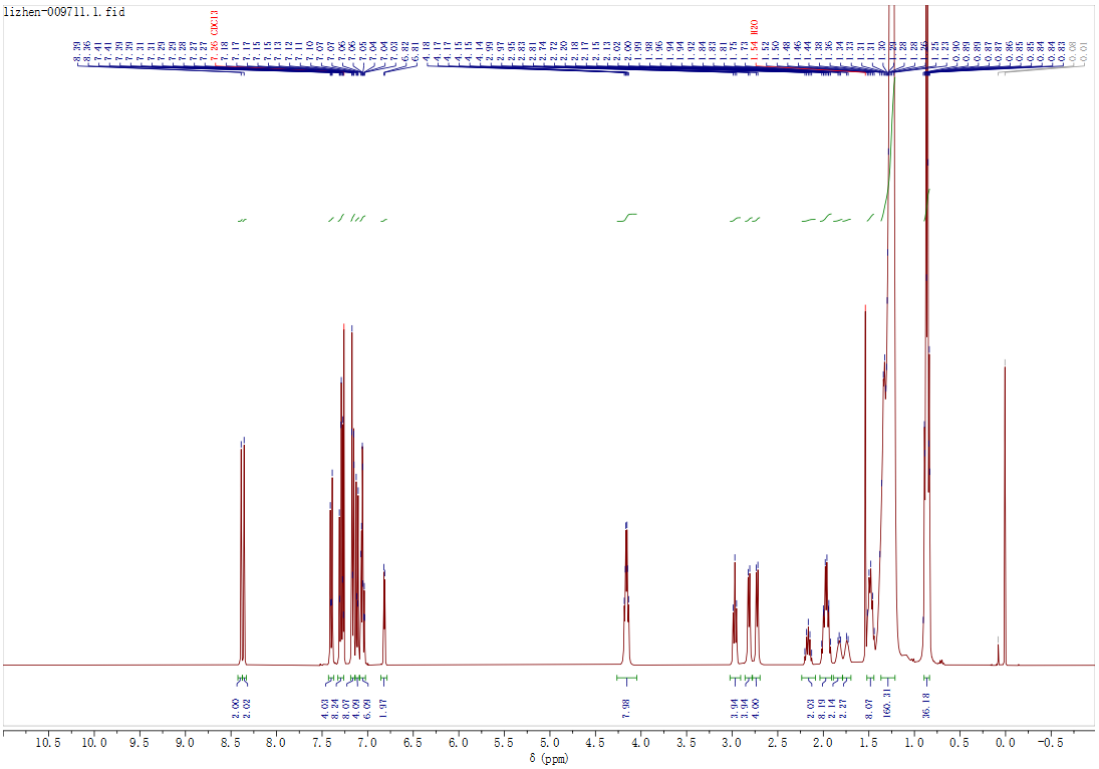

Figure S5. ^{1}H NMR spectrum of HD-C3 (400 MHz, $CDCl_3$).

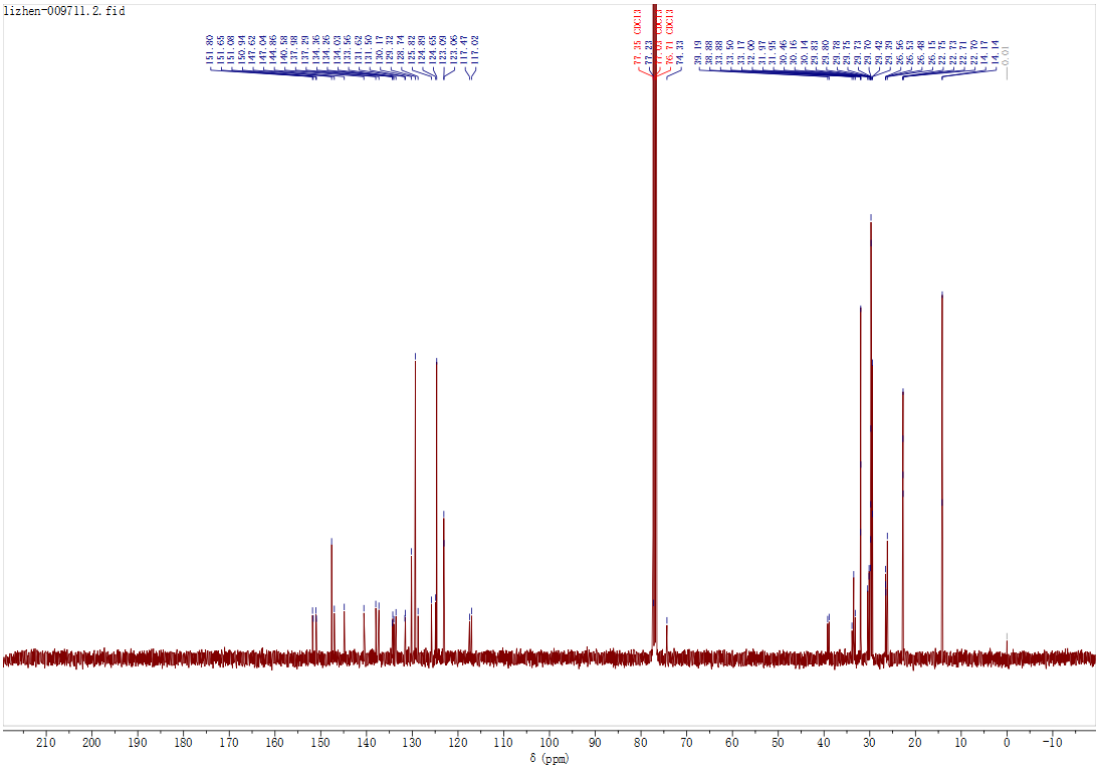

Figure S6. ^{13}C NMR spectrum of HD-C3 (101 MHz, $CDCl_3$).

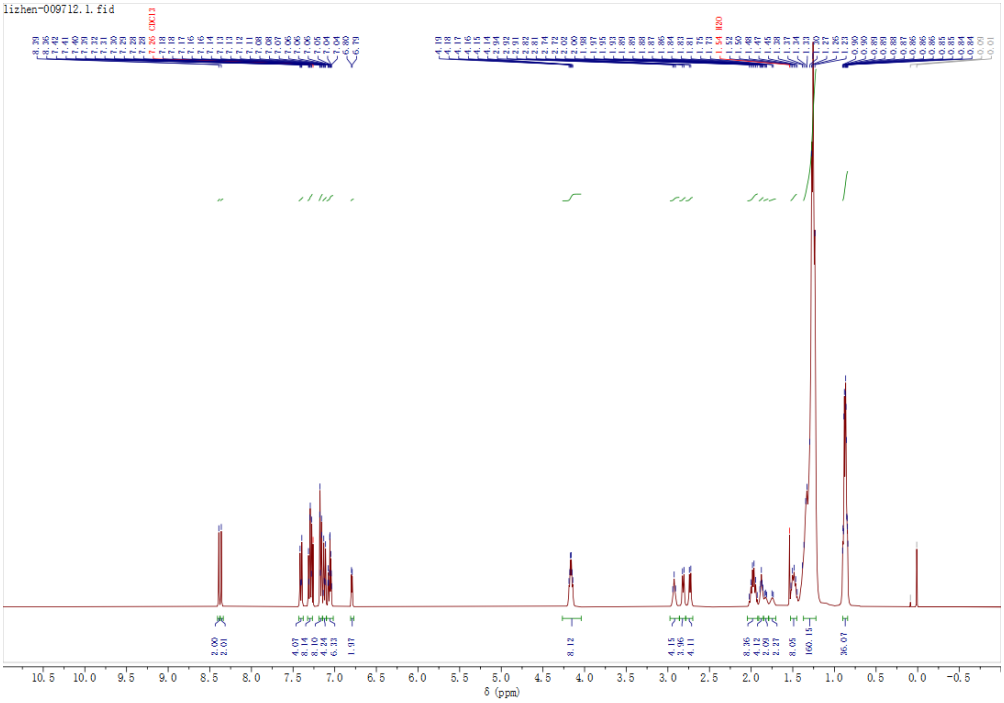

Figure S7. ^{1}H NMR spectrum of HD-C4 (400 MHz, $CDCl_3$).

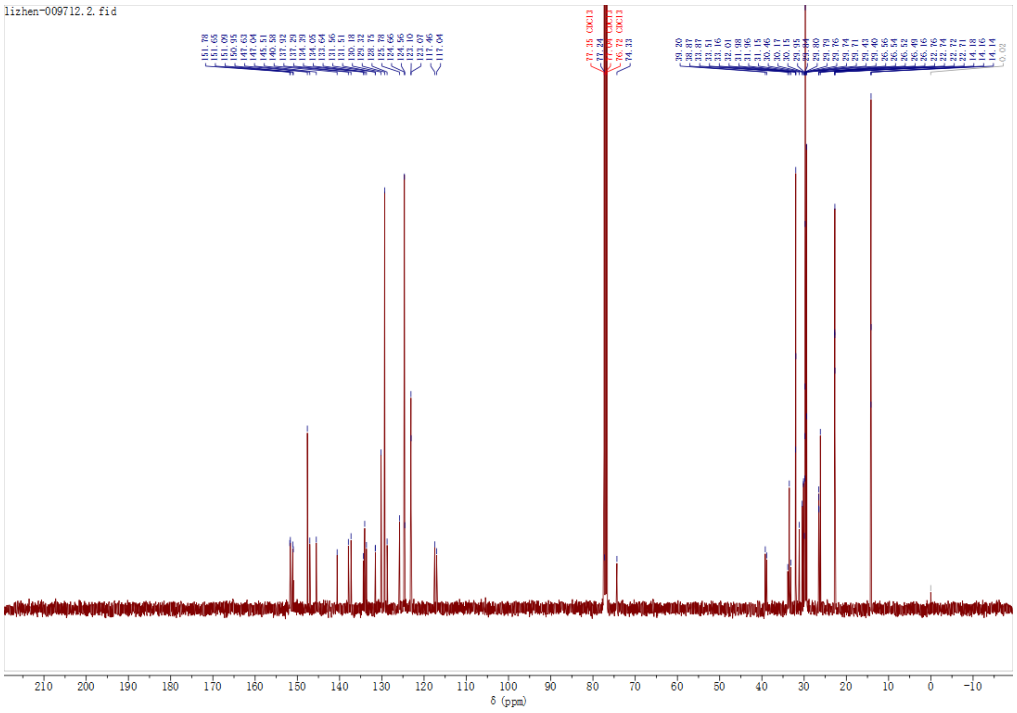

Figure S8. ^{13}C NMR spectrum of HD-C4 (101 MHz, $CDCl_3$).

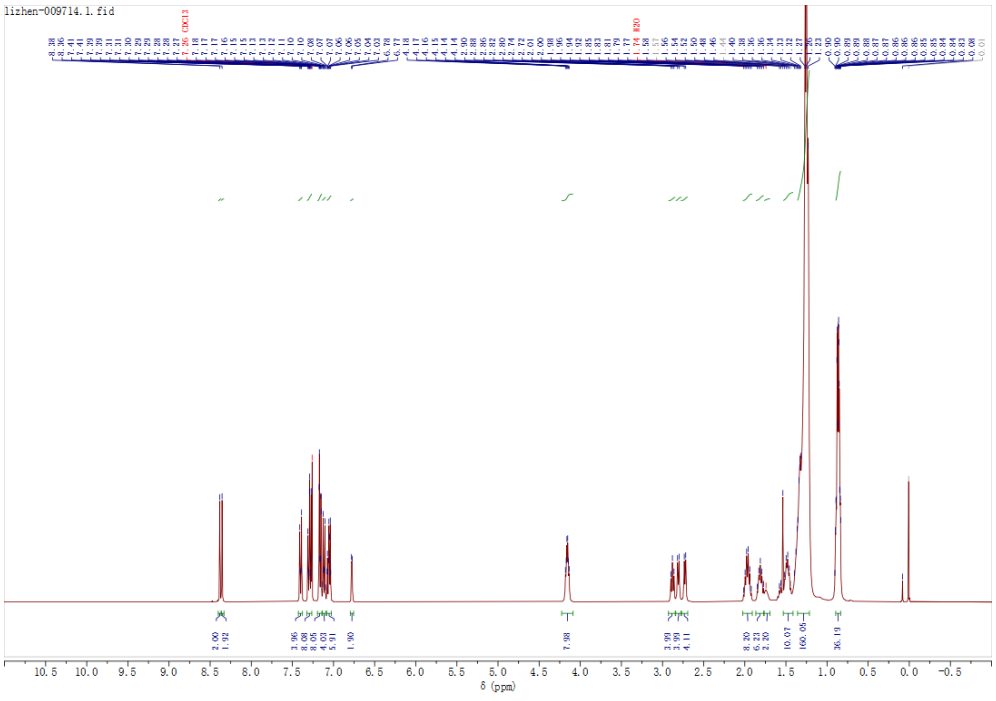

Figure S9. ^{1}H NMR spectrum of HD-C5 (400 MHz, $CDCl_3$).

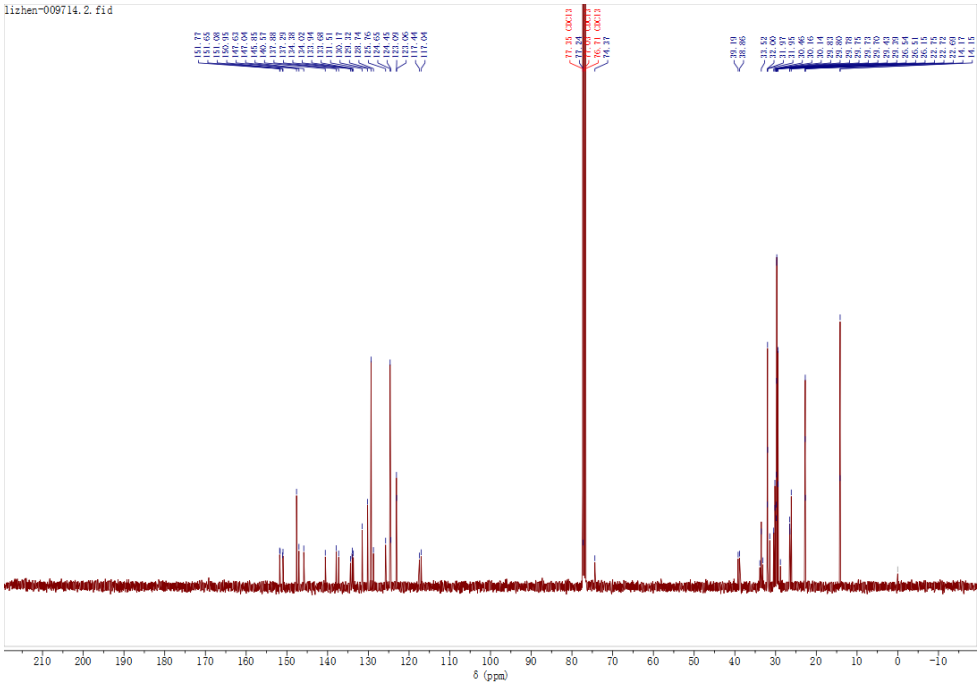

Figure S10. ^{13}C NMR spectrum of HD-C5 (101 MHz, $CDCl_3$).

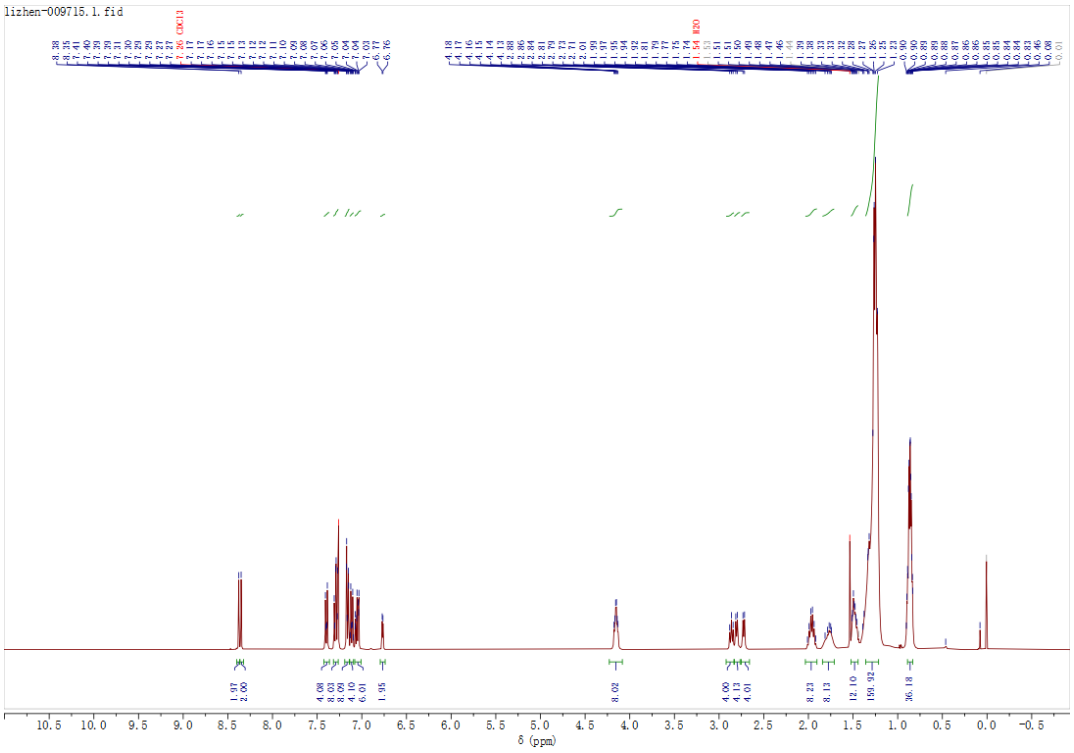

Figure S11. ^{1}H NMR spectrum of HD-C6 (400 MHz, $CDCl_3$).

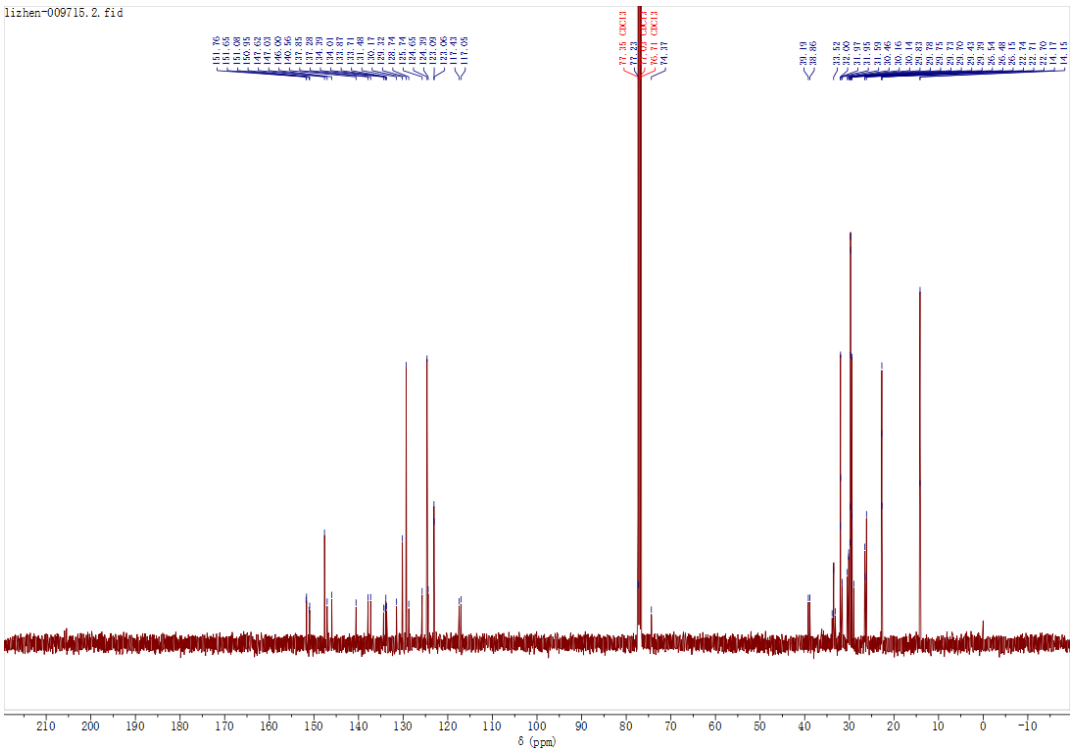

Figure S12. ^{13}C NMR spectrum of HD-C6 (101 MHz, $CDCl_3$).

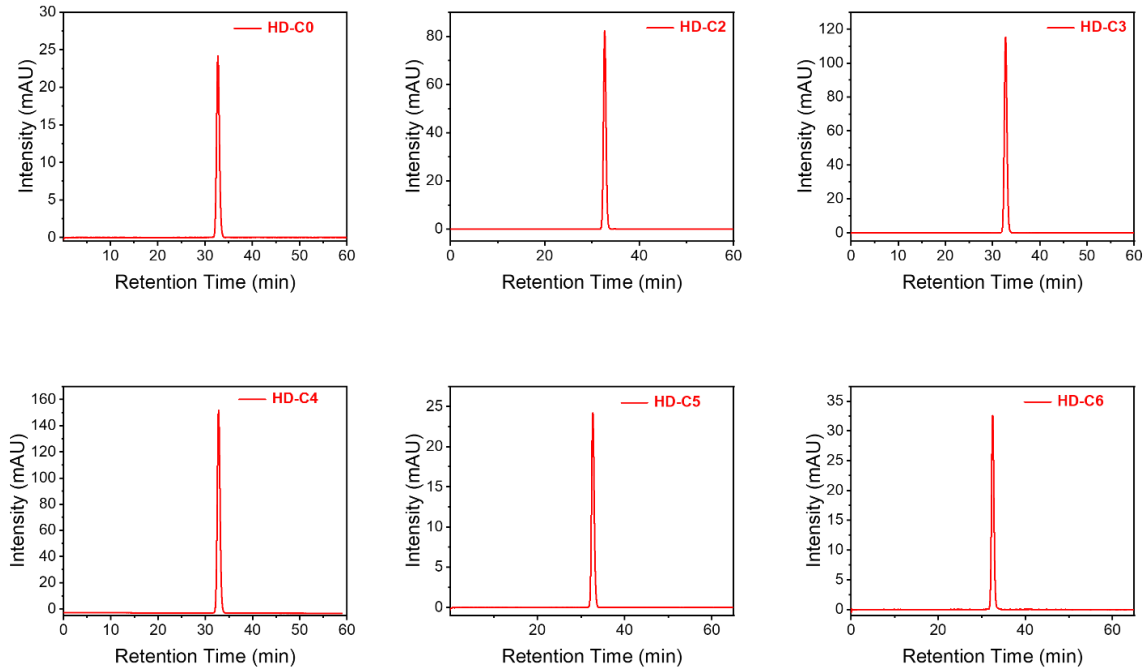

Figure S13. HPLC curves of organic dyes (THF as eluant, 6 mL min^{-1} programmed flow).

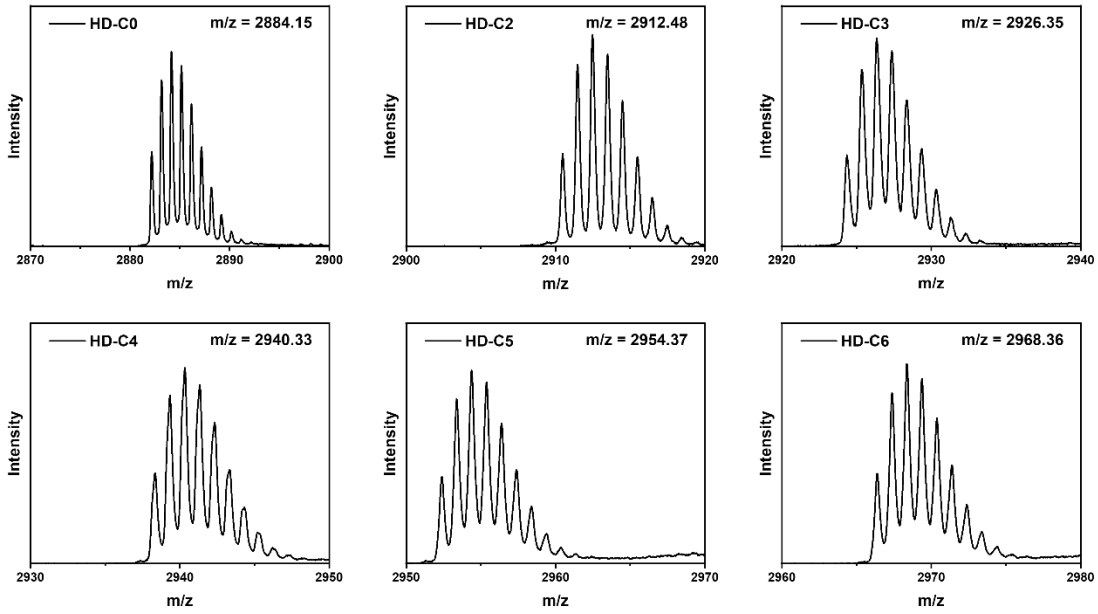

Figure S14. MALDI-TOF spectra of organic dyes.

Photophysical property of organic dyes

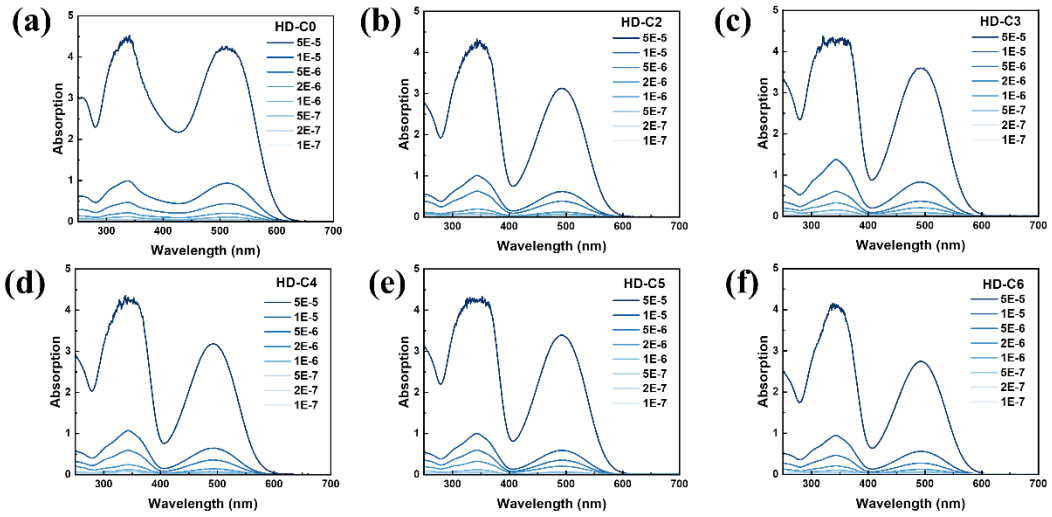

Figure S15. The UV-vis absorption spectra of dyes with different concentrations ranging from 1×10^{-7} mol L^{-1} to 5×10^{-5} mol L^{-1} in dichloromethane solution.

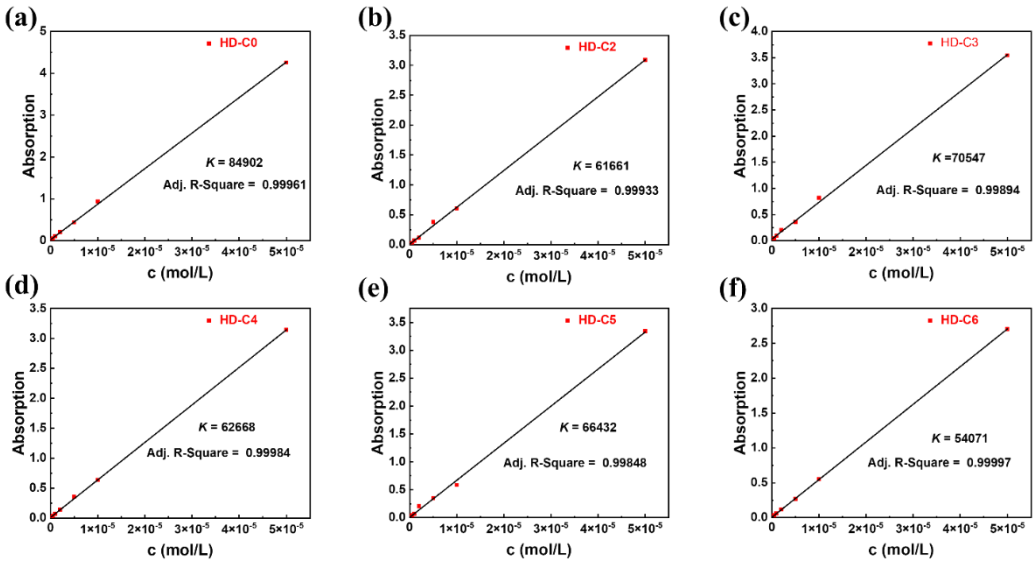

Figure S16. The molar extinction coefficient fitting curves at λ_{abs} in the visible light region of dyes in the dichloromethane solution.

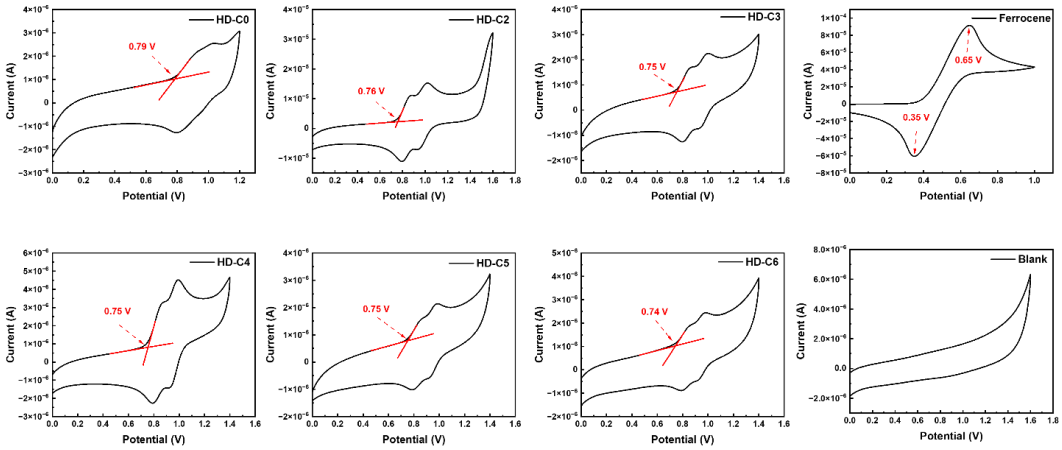

Figure S17. Cyclic voltammetry curves of dyes in dichloromethane solution with concentrations at 1×10^{-6} mol L^{-1} (Ag/AgCl electrode, tetrabutylammonium hexafluorophosphate as electrolyte, ferrocene as internal standard, scan speed: 0.10 V s^{-1}).

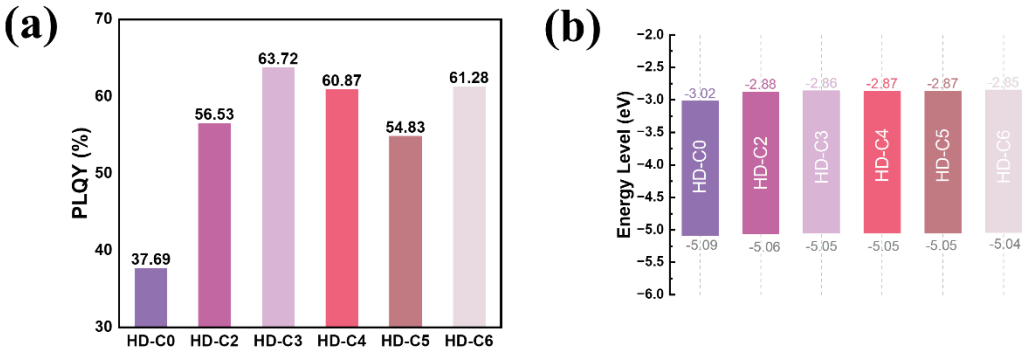

Figure S18. (a) PLQYs of dyes in the solid states. (b) Energy levels calculated from CV curves of dyes in the dichloromethane solution with a concentration of 1×10^{-6} mol L^{-1}.

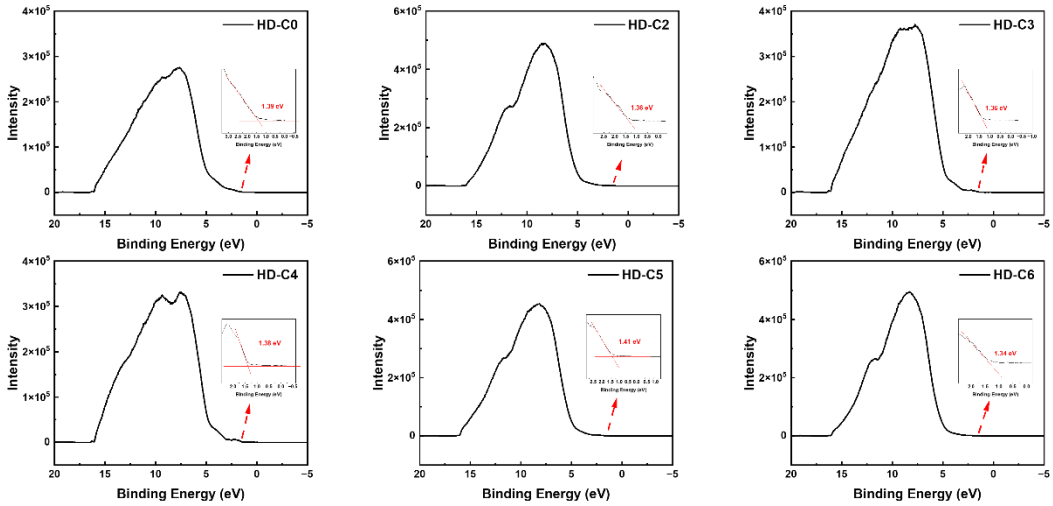

Figure S19. Ultraviolet Photoelectron Spectroscopy (UPS) of dyes with no bias.

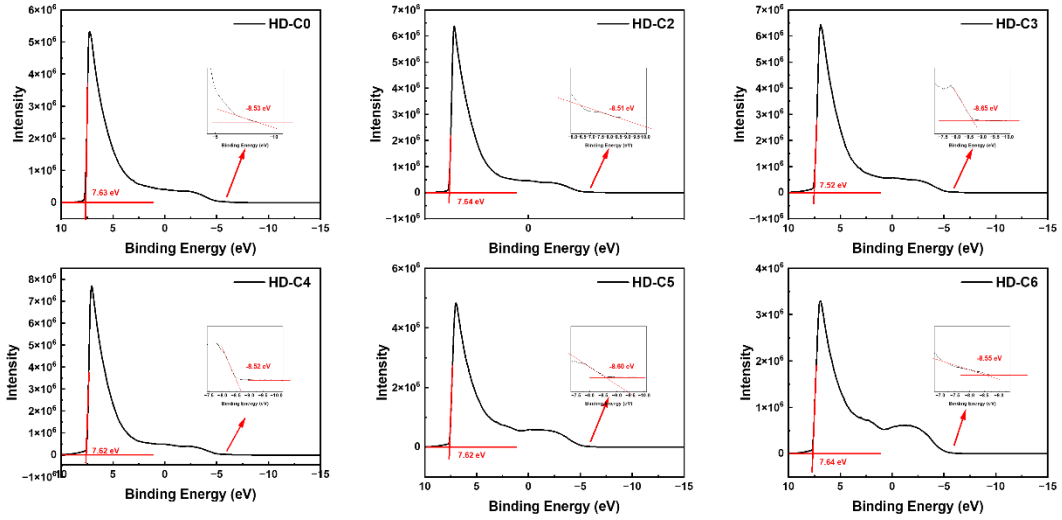

Figure S20. Ultraviolet Photoelectron Spectroscopy (UPS) of dyes with a -10 V bias. HOMO energy levels are calculated according to the following equation: E_{HOMO} (*vs.* vacuum conditions) = – (E_{photon} – width of UPS spectra), where E_{photon} denotes the excitation energy of He I (21.220 eV).

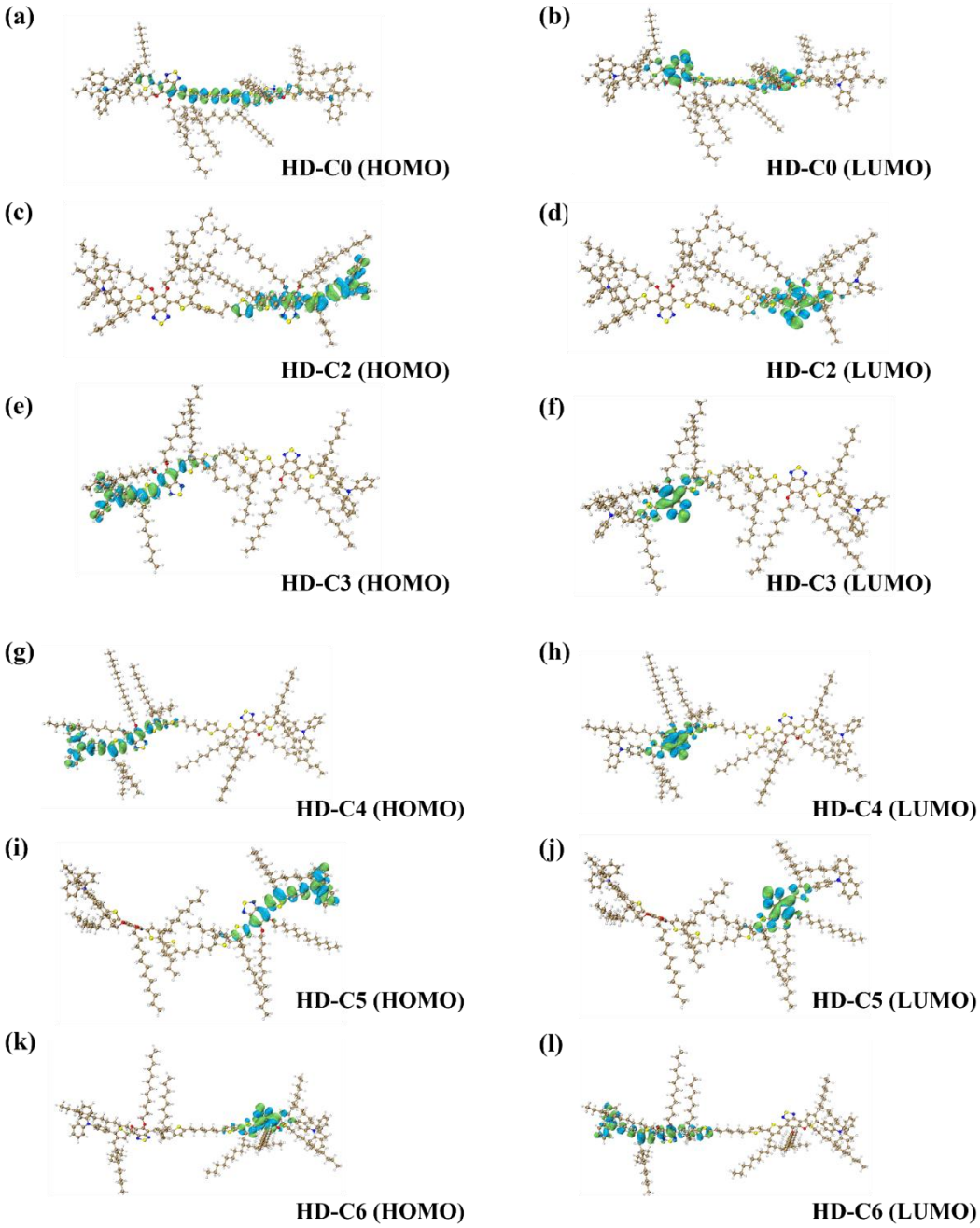

Figure S21. Optimized molecular configurations and frontier orbital distribution of organic dyes.

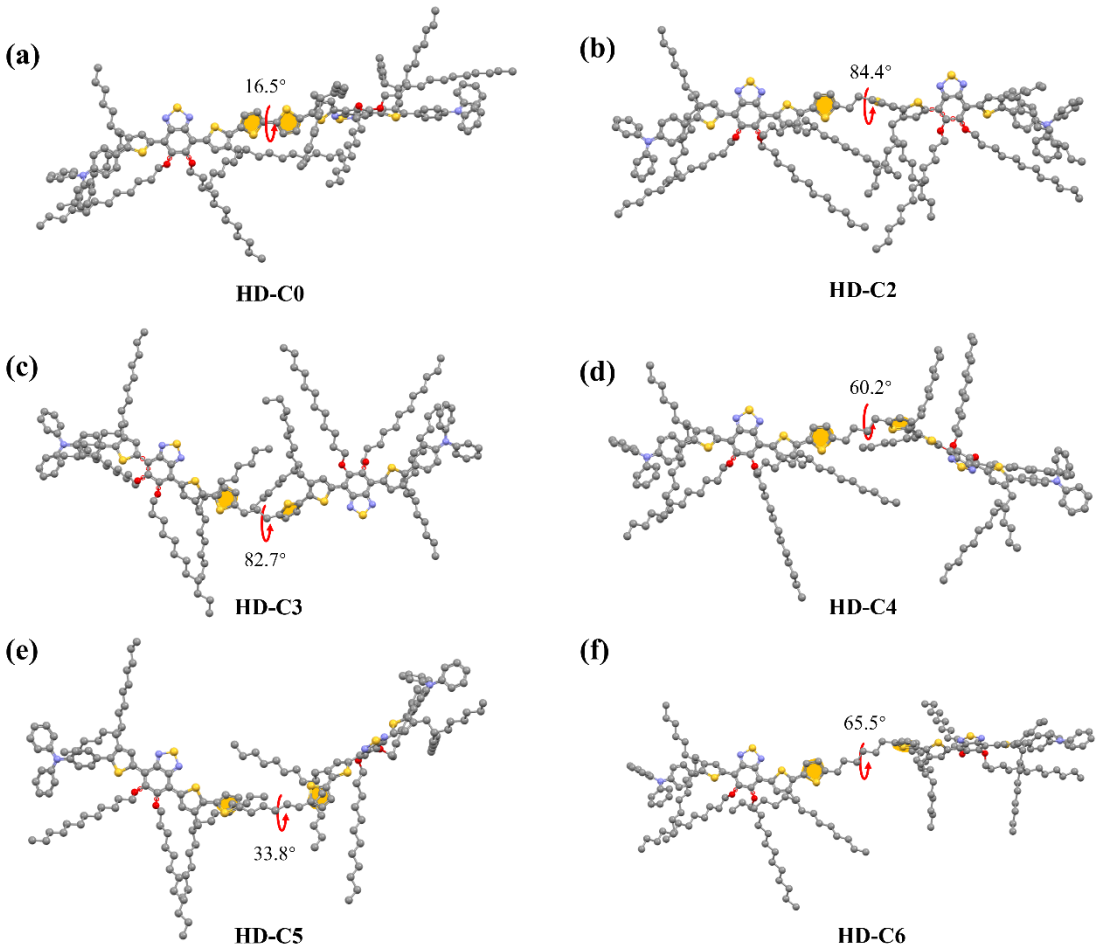

Figure S22. The optimized molecular geometries of dyes and the corresponding dihedral angle between thiophene bridges.

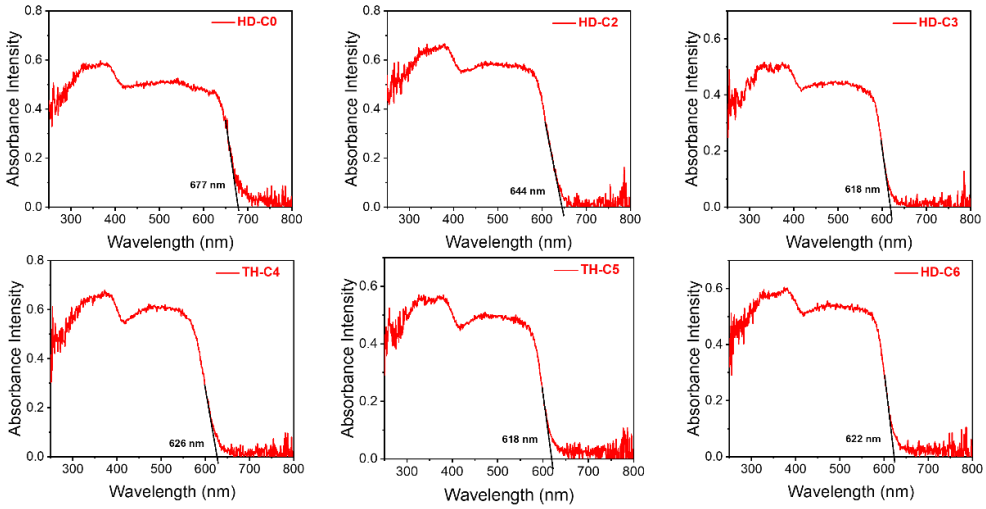

Figure S23. UV–Vis DRS absorption spectra of dyes in the solid state.

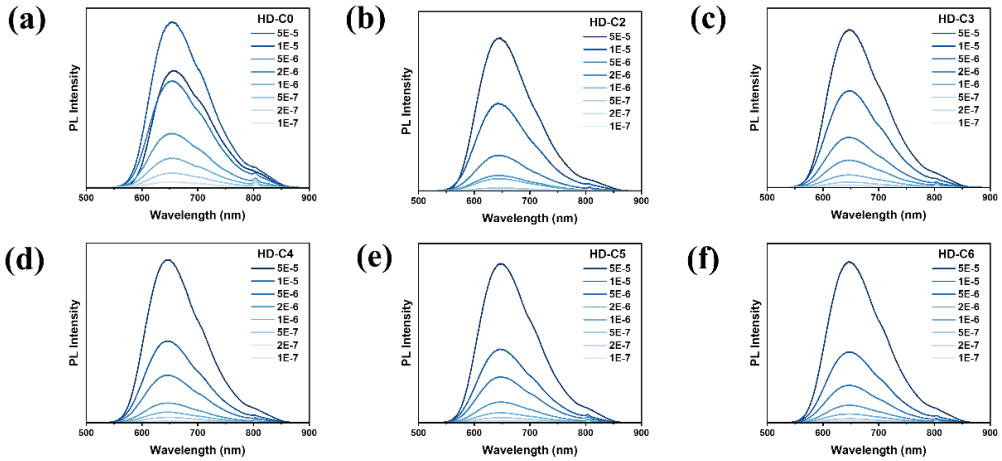

Figure S24. The photoluminescence spectra of dyes in diluted dichloromethane solution with concentrations ranging from 1×10^{-7} mol L^{-1} to 5×10^{-5} mol L^{-1}.

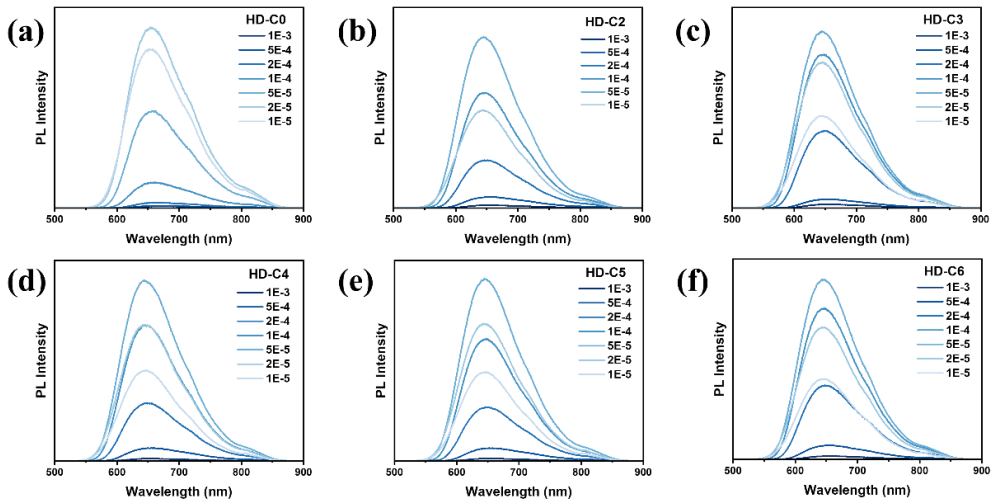

Figure S25. The photoluminescence spectra of dyes in dichloromethane solution with concentrations ranging from 1×10^{-5} mol L^{-1} to 5×10^{-3} mol L^{-1}.

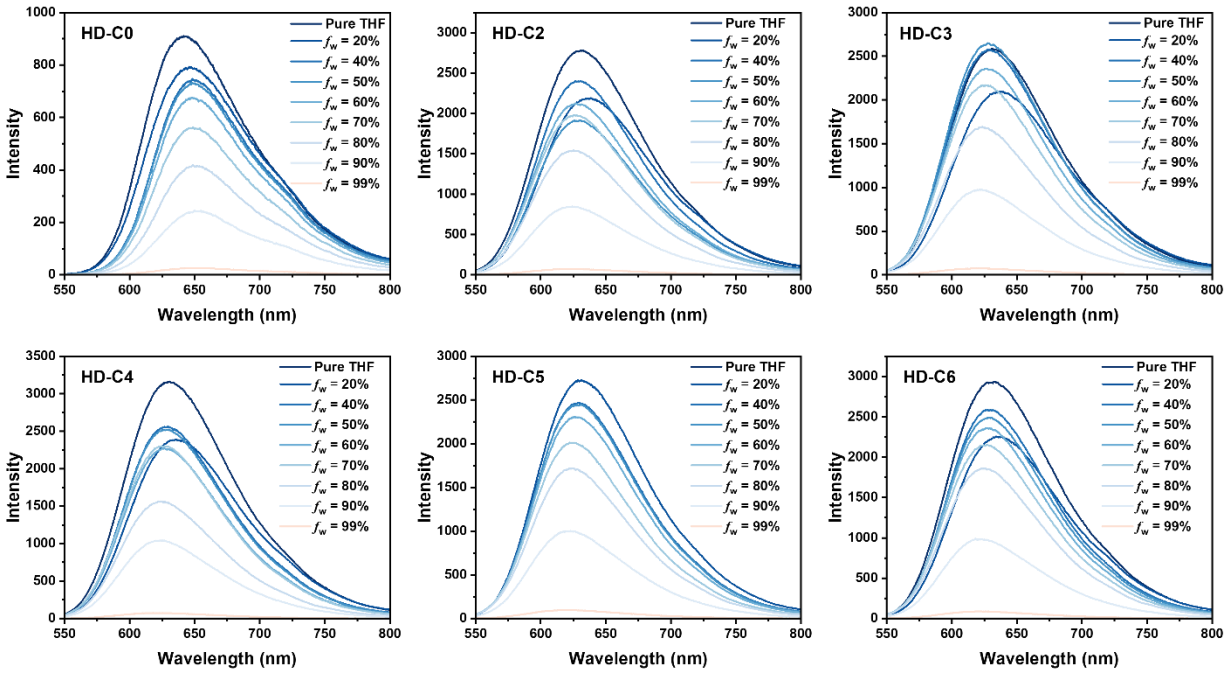

Figure S26. Fluorescence spectra of dyes in different ratios of water (f_w) from 0% to 99% in THF/H_2O mixture.

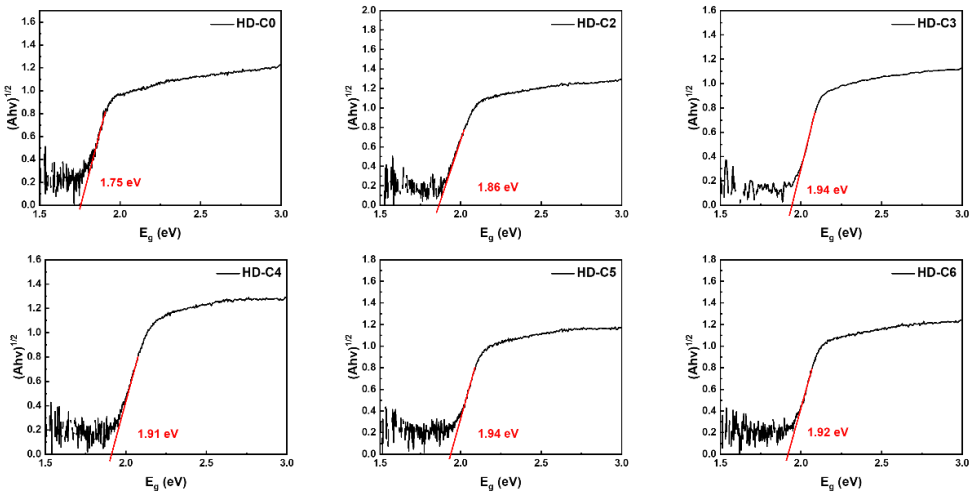

Figure S27. The bandgaps of dyes in the solid state calculated by the Tauc-plot.

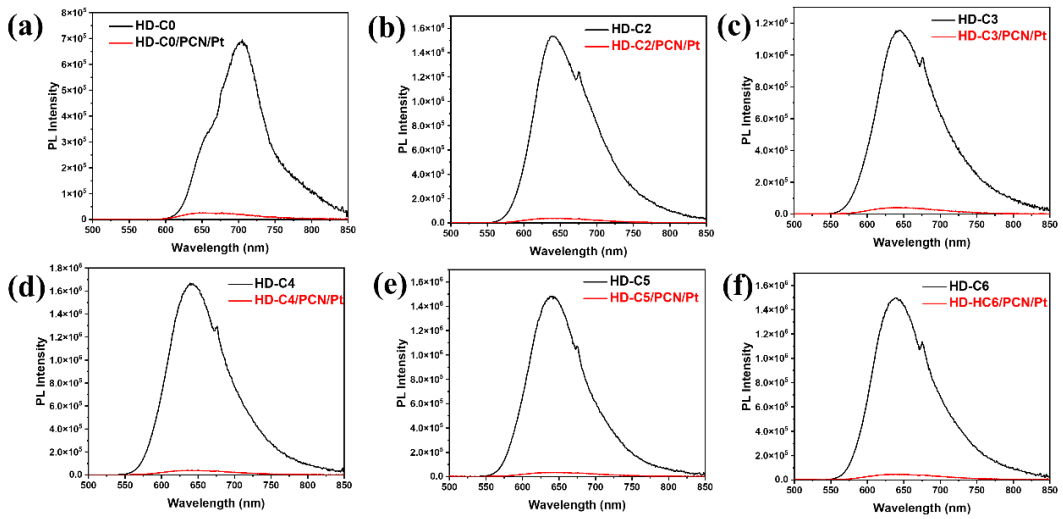

Figure S28. Photoluminescence spectra of dyes in the solid state and dyes/PCN/Pt systems.

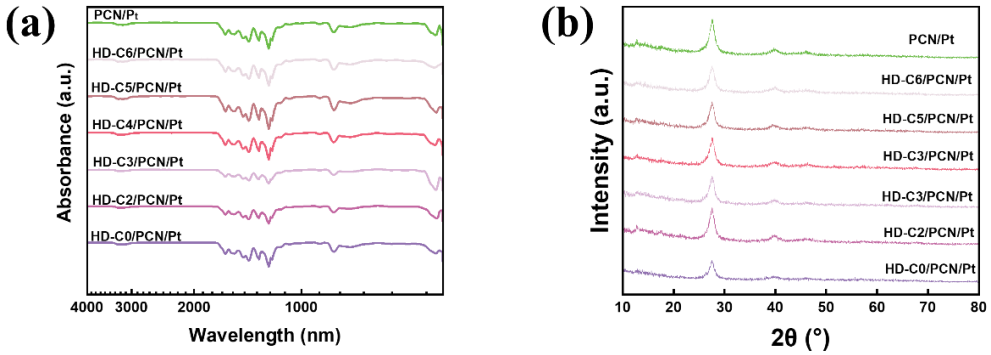

Figure S29. (a) FTIR spectra of PCN/Pt and dyes/PCN/Pt in their powder state. (b) XRD spectra of PCN/Pt and dyes/PCN/Pt in their powder state.

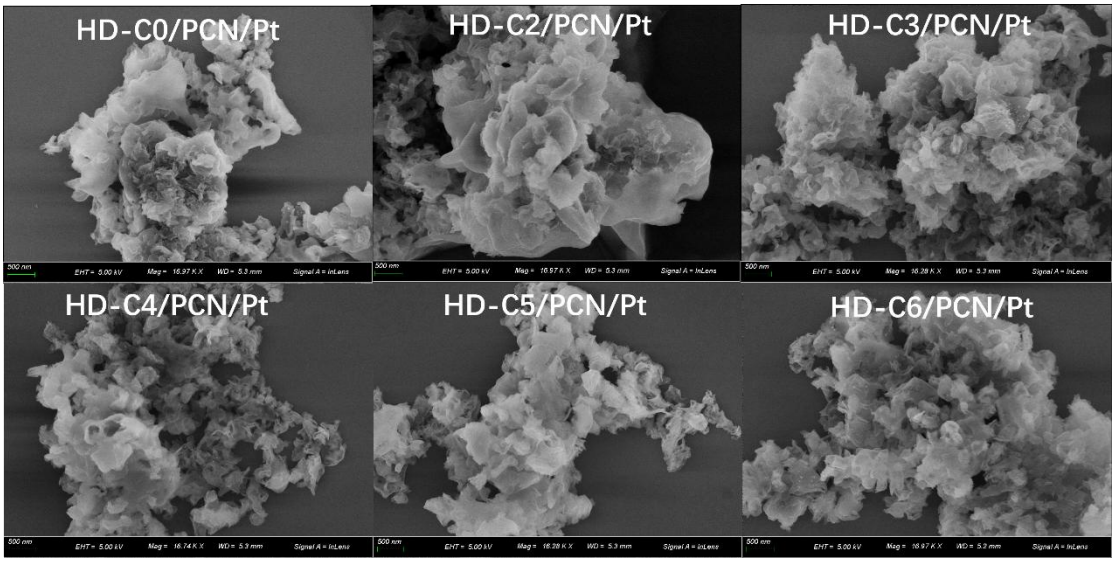

Figure S30. SEM images of dyes/PCN/Pt.

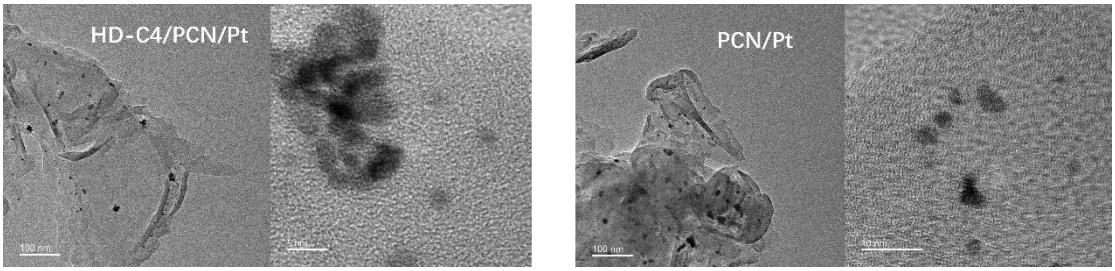

Figure S31. HR-TEM images of dyes/PCN/Pt.

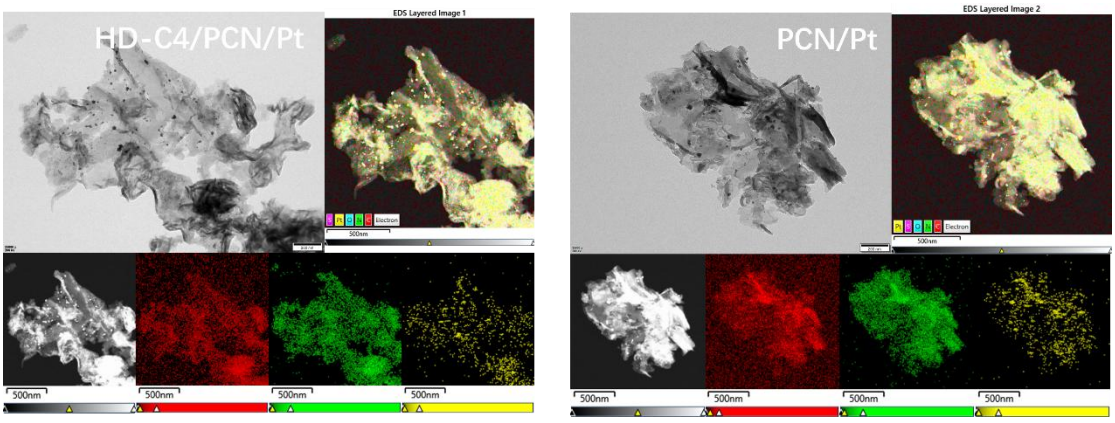

Figure S32. HAADF-STEM images of dyes/PCN/Pt.

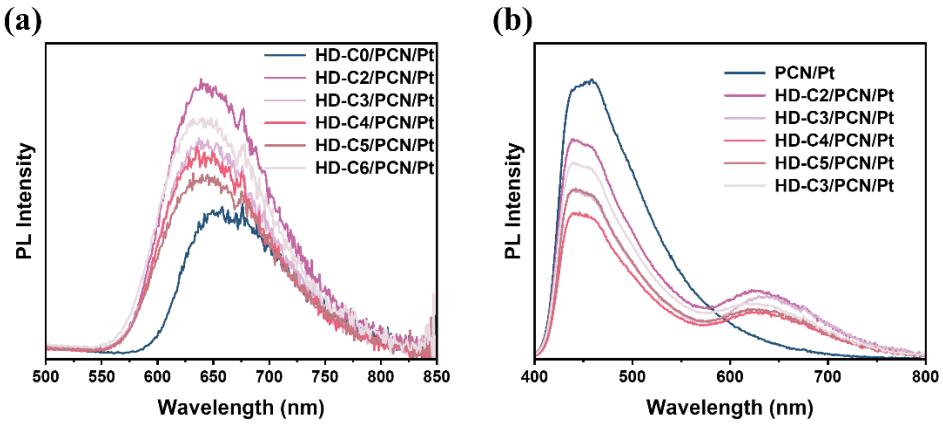

Figure S33. Photoluminescence spectra of dyes/PCN/Pt in powder state (a) λ_{ex}: 450 nm. (b) λ_{ex}: 350 nm.

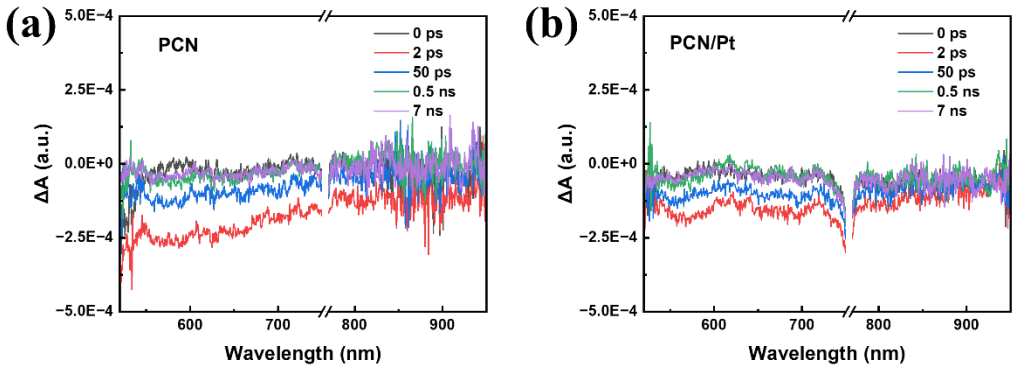

Figure S34. Transient absorption spectra of PCN and PCN/Pt in their powder state.

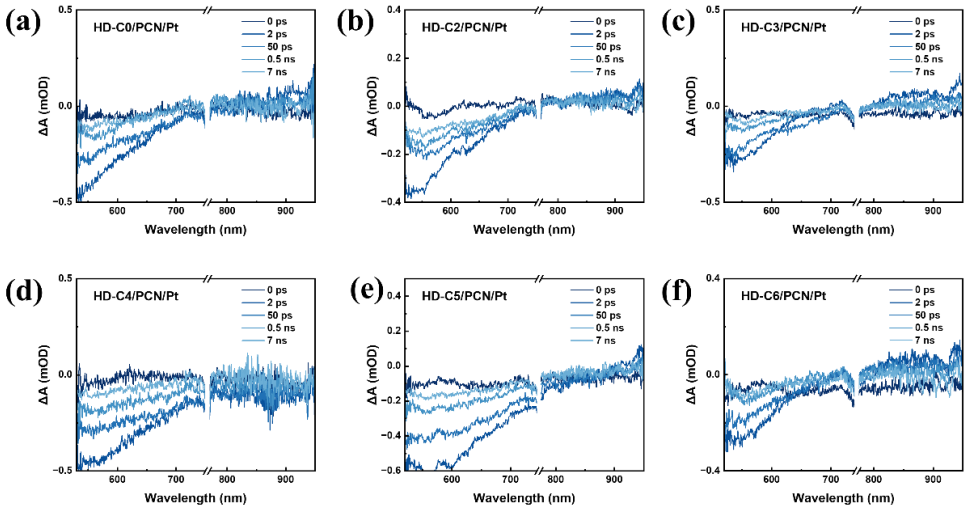

Figure S35. Transient absorption spectra of dyes/PCN/Pt in their powder state.

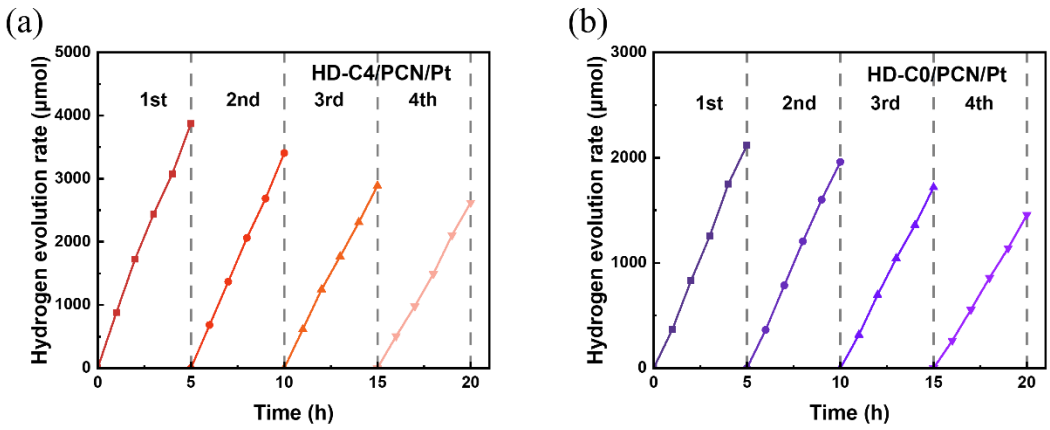

Figure S36. Stability measurements of (a) HD-C4/PCN/Pt and (b) HD-C0/PCN/Pt under visible-light irradiation (50 mg photocatalyst, 10 mL TEOA, 100 mL H_2O, and a 300 W Xe lamp with a cut-off filter $\geqslant$ 420 nm).

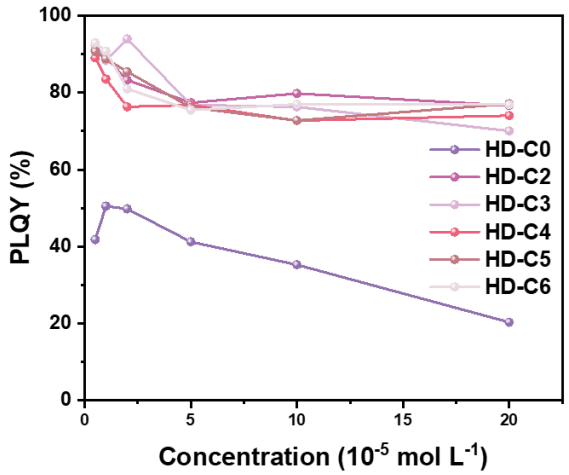

Figure S37. Photoluminescence quantum yields (PLQYs) of HD-Cn dyes at different concentrations in dichloromethane solution.

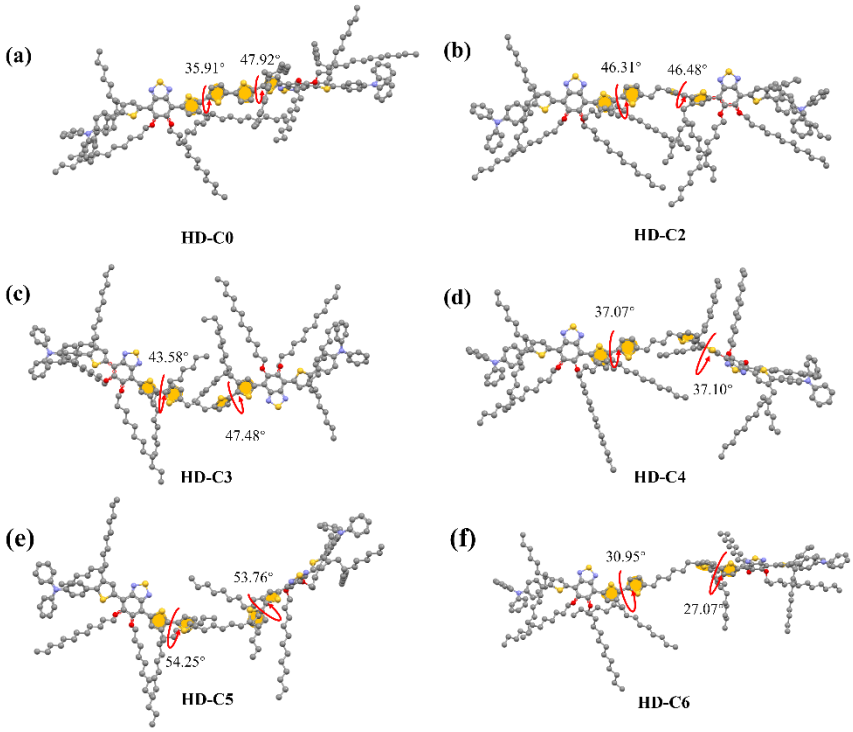

Figure S38. Dihedral angle measurement results between the two thiophene rings at the junction connecting the dye molecular fragment and the conjugated linkage unit.

Table S1 The hydrogen production performance of PCN-based photocatalysts

structures	Sacrificial agent	Light Source	PHE rates (mmol/g/h)	Reference
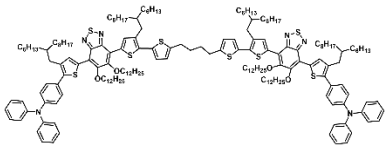	TEOA	⩾ 420 nm	17.2	This work
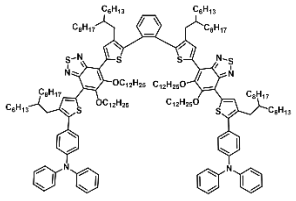	TEOA	⩾ 420 nm	16.7	5
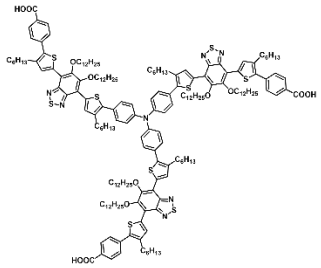	TEOA	⩾ 420 nm	19.9	6

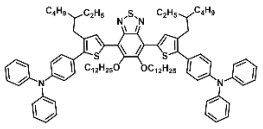	TEOA	⩾ 420 nm	11.9	7
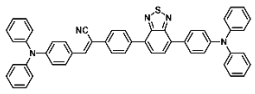	TEOA	⩾ 420 nm	20.1	8
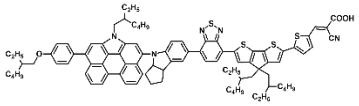	AA	⩾ 420 nm	11.9	9
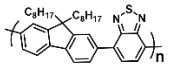	TEOA	⩾ 420 nm	0.7	10
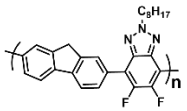	TEOA	⩾ 420 nm	14.9	11
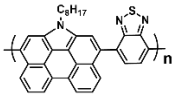	TEOA	⩾ 420 nm	13.0	12
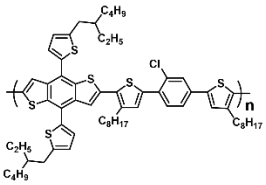	TEOA	⩾ 420 nm	111.8	13
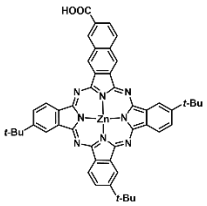	AA	⩾ 500 nm	1.3	14

Reference

1. Gaussian 16, M. J. Frisch, G. W. Trucks, H. B. Schlegel, G. E. Scuseria, M. A. Robb, J. R. Cheeseman, G. Scalmani, V. Barone, G. A. Petersson, H. Nakatsuji, X. Li, M. Caricato, A. V. Marenich, J. Bloino, B. G. Janesko, R. Gomperts, B. Mennucci, H. P. Hratchian, J. V. Ortiz, A. F. Izmaylov, J. L. Sonnenberg, Williams, F. Ding, F. Lipparini, F. Egidi, J. Goings, B. Peng, A. Petrone, T. Henderson, D. Ranasinghe, V. G. Zakrzewski, J. Gao, N. Rega, G. Zheng, W. Liang, M. Hada, M. Ehara, K. Toyota, R. Fukuda, J. Hasegawa, M. Ishida, T. Nakajima, Y. Honda, O. Kitao, H. Nakai, T. Vreven, K. Throssell, J. A. Montgomery Jr., J. E. Peralta, F. Ogliaro, M. J. Bearpark, J. J. Heyd, E. N. Brothers, K. N. Kudin, V. N. Staroverov, T. A. Keith, R. Kobayashi, J. Normand, K. Raghavachari, A. P. Rendell, J. C. Burant, S. S. Iyengar, J. Tomasi, M. Cossi, J. M. Millam, M. Klene, C. Adamo, R. Cammi, J. W. Ochterski, R. L. Martin, K. Morokuma, O. Farkas, J. B. Foresman and D. J. Fox, Gaussian, Inc., Wallingford CT, 2016.
2. T. Lu and F. Chen, J. Comput. Chem., 2012, 33, 580.
3. W. Humphrey., A. Dalke. and K. Schulten., J. Mol. Graph., 1996, 14, 33.
4. F. Qi, Y. Li, R. Zhang, F. R. Lin, K. Liu, Q. Fan and A. K. Jen, Angew. Chem. Int. Ed., 2023, 62, e202303066.
5. Y. Chen, C. Jiang, S. Liu, W. Yuan, Q. Li and Z. Li, Angew. Chem. Int. Ed., 2025, 64, e202419850.
6. S. Liu, P. Lin, M. Wu, Z.-A. Lan, H. Zhuzhang, M. Han, Y. Fan, X. Chen, X. Wang, Q. Li and Z. Li, Appl. Catal. B Environ., 2022, 309, 121257.
7. S. Liu, Q. Chen, Y. Chen, P. Lin, H. Zhuzhang, M. Han, Z.-A. Lan, X. Chen, X. Wang, Q. Li and Z. Li, J. Mater. Chem. A., 2023, 11, 14682.
8. K. Li, L. Wang, Z. Chen, X. Yang, Y. X. Yu, W. D. Zhang, Y. Wang, Y. Shi, K. P. Loh and Q. H. Xu, Adv. Funct. Mater., 2020, 30, 2005106.
9. F. Yu, Z. Wang, S. Zhang, K. Yun, H. Ye, X. Gong, J. Hua and H. Tian, Appl. Catal. B Environ., 2018, 237, 32.
10. J. Chen, C. L. Dong, D. Zhao, Y. C. Huang, X. Wang, L. Samad, L. Dang, M. Shearer, S. Shen and L. Guo, Adv. Mater., 2017, 29, 1606198.
11. H. Ye, Z. Wang, F. Yu, S. Zhang, K. Kong, X. Gong, J. Hua and H. Tian, Appl. Catal. B Environ., 2020, 267, 118577.
12. F. Yu, Z. Wang, S. Zhang, H. Ye, K. Kong, X. Gong, J. Hua and H. Tian, Adv. Funct. Mater., 2018, 28, 1804512.
13. L. Xu, B. Tian, T. Wang, Y. Yu, Y. Wu, J. Cui, Z. Cao, J. Wu, W. Zhang, Q. Zhang, J. Liu, Z. Li and Y. Tian, Energy Environ. Sci., 2022, 15, 5059.
14. X. Zhang, L. Yu, C. Zhuang, T. Peng, R. Li and X. Li, ACS Catal., 2013, 4, 162.